SATELLITE REMOTE SENSING OF SEA SURFACE TEMPERATURES

P. J. Minnett, University of Miami, Miami, FL, USA

doi:10.1006/rwos.2001.0343

Introduction

The ocean surface is the interface between the two dominant, fluid components of the Earth's climate system: the oceans and atmosphere. The heat moved around the planet by the oceans and atmosphere helps make much of the Earth's surface habitable, and the interactions between the two, that take place through the interface, are important in shaping the climate system. The exchange between the ocean and atmosphere of heat, moisture, and gases (such as CO_2) are determined, at least in part, by the sea surface temperature (SST). Unlike many other critical variables of the climate system, such as cloud cover, temperature is a well-defined physical variable that can be measured with relative ease. It can also be measured to useful accuracy by instruments on observation satellites.

The major advantage of satellite remote sensing of SST is the high-resolution global coverage provided by a single sensor, or suite of sensors on similar satellites, that produces a consistent data set. By the use of onboard calibration, the accuracy of the time-series of measurements can be maintained over years, even decades, to provide data sets of relevance to research into the global climate system. The rapid processing of satellite data permits the use of the global-scale SST fields in applications where the immediacy of the data is of prime importance, such as weather forecasting – particularly the prediction of the intensification of tropical storms and hurricanes.

Measurement Principle

The determination of the SST from space is based on measuring the thermal emission of electromagnetic radiation from the sea surface. The instruments, called radiometers, determine the radiant energy flux, B_λ, within distinct intervals of the electromagnetic spectrum. From these the brightness temperature (the temperature of a perfectly emitting 'black-body' source that would emit the same radiant flux) can be calculated by the Planck equation:

$$B_\lambda(T) = 2hc^2\lambda^{-5}(e^{hc/(\lambda kT)} - 1)^{-1} \quad [1]$$

where h is Planck's constant, c is the speed of light in a vacuum, k is Boltzmann's constant, λ is the wavelength and T is the temperature. The spectral intervals (wavelengths) are chosen where three conditions are met: (1) the sea emits a measurable amount of radiant energy, (2) the atmosphere is sufficiently transparent to allow the energy to propagate to the spacecraft, and (3) current technology exists to build radiometers that can measure the energy to the required level of accuracy within the bounds of size, weight, and power consumption imposed by the spacecraft. In reality these constrain the instruments to two relatively narrow regions of the infrared part of the spectrum and to low-frequency microwaves. The infrared regions, the so-called atmospheric windows, are situated between wavelengths of 3.5–4.1 μm and 8–12 μm (**Figure 1**); the microwave measurements are made at frequencies of 6–12 GHz.

As the electromagnetic radiation propagates through the atmosphere, some of it is absorbed and scattered out of the field of view of the radiometer, thereby attenuating the original signal. If the attenuation is sufficiently strong none of the radiation from the sea reaches the height of the satellite, and such is the case when clouds are present in the field of view of infrared radiometers. Even in clear-sky conditions a significant fraction of the sea surface emission is absorbed in the infrared windows. This energy is re-emitted, but at a temperature characteristic of that height in the atmosphere. Consequently the brightness temperatures measured through the clear atmosphere by a spacecraft radiometer are cooler than would be measured by a similar device just above the surface. This atmospheric effect, frequently referred to as the temperature deficit, must be corrected accurately if the derived sea surface temperatures are to be used quantitatively.

Infrared Atmospheric Correction Algorithms

The peak of the Planck function for temperatures typical of the sea surface is close to the longer wavelength infrared window, which is therefore well suited to SST measurement (**Figure 1**). However, the main atmospheric constituent in this spectral interval that contributes to the temperature

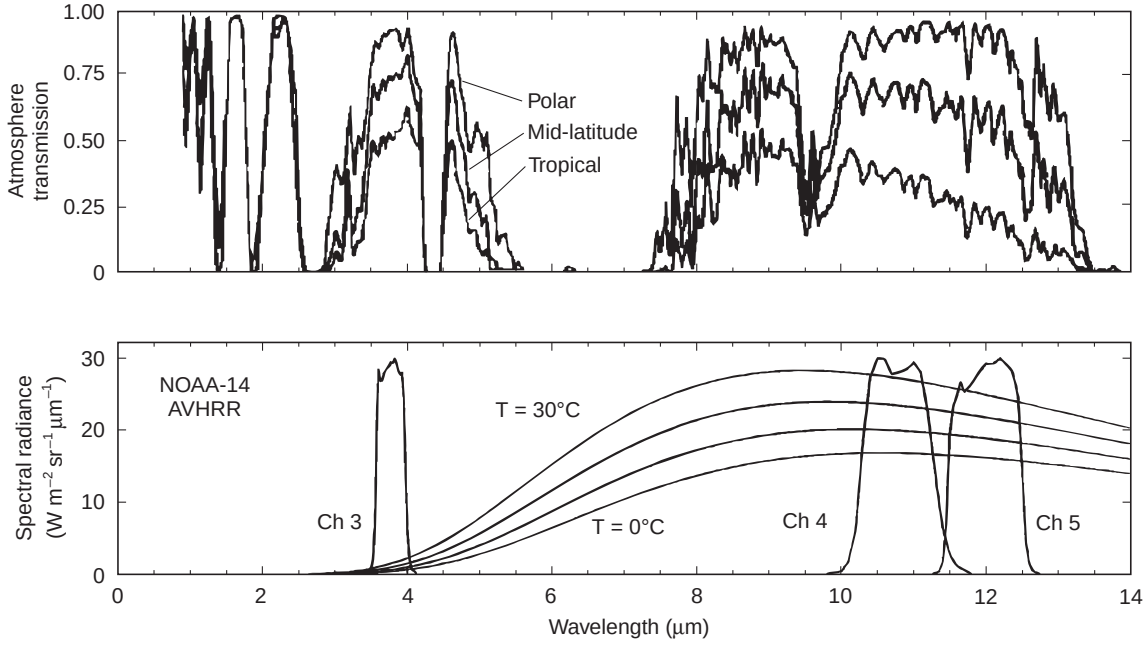

Figure 1 Spectra of atmospheric transmission in the infrared (wavelengths 1–14 μm) calculated for three typical atmospheres from diverse parts of the ocean; polar, mid-latitude and tropical with integrated water vapor content of 7 kg m^{-2} (polar), 29 kg m^{-2} (mid-latitude) and 54 kg m^{-2} (tropical). Regions where the transmission is high are well suited to satellite remote sensing of SST. The lower panel shows the electromagnetic radiative flux for four sea surface temperatures (0, 10, 20, and 30°C) with the relative spectral response functions for channels 3, 4, and 5 of the AVHRR on the NOAA-14 satellite. The so-called 'split-window' channels, 4 and 5, are situated where the sea surface emission is high, and where the atmosphere is comparatively clear but exhibits a strong dependence on atmospheric water vapor content.

deficit is water vapor, which is very variable both in space and time. Other molecular species that contribute to the temperature deficit are quite well mixed throughout the atmosphere, and therefore inflict a relatively constant temperature deficit that is simple to correct.

The variability of water vapor requires an atmospheric correction algorithm based on the information contained in the measurements themselves. This is achieved by making measurements at distinct spectral intervals in the windows when the water vapor attenuation is different. These spectral intervals are defined by the characteristics of the radiometer and are usually referred to as bands or channels (**Figure 1**). By invoking the hypothesis that the difference in the brightness temperatures measured in two channels, i and j, is related to the temperature deficit in one of them, the atmospheric correction algorithm can be formulated thus:

$$SST_{ij} - T_i = f(T_i - T_j) \qquad [2]$$

where SST_{ij} is the derived SST and T_i, T_j are the brightness temperatures in channels i, j.

Further, by assuming that the atmospheric attenuation is small in these channels, so that the radiative transfer can be linearized, and that the channels are spectrally close so that Planck's function can be linearized, the algorithm can be expressed in the very simple form:

$$SST_{ij} = a_o + a_i T_i + a_j T_j \qquad [3]$$

where are a_o, a_i, and a_j are coefficients. These are determined by regression analysis of either coincident satellite and *in situ* measurements, mainly from buoys, or of simulated satellite measurements derived by radiative transfer modeling of the propagation of the infrared radiation from the sea surface through a representative set of atmospheric profiles.

The simple algorithm has been applied for many years in the operational derivation of the sea surface from measurements of the Advanced Very High Resolution Radiometer (AVHRR, see below), the product of which is called the multi-channel SST (MCSST), where i refers to channel 4 and j to channel 5.

More complex forms of the algorithms have been developed to compensate for some of the shortcomings of the linearization. One such widely applied algorithm takes the form:

$$SST_{ij} = b_o + b_1 T_i + b_2 (T_i - T_j) SST_r + b_3 (T_i - T_j)(\sec\theta - 1) \qquad [4]$$

where SST_r is a reference SST (or first-guess temperature), and θ is the zenith angle to the satellite radiometer measured at the sea surface. When applied to AVHRR data, with i and j referring to channels 4 and 5 derived SST is called the nonlinear SST (NLSST). A refinement is called the Pathfinder SST (PFSST) in the research program designed to post-process AVHRR data over a decade or so to provide a consistent data set for climate research. In the PFSST, the coefficients are derived on a monthly basis for two different atmospheric regimes, distinguished by the value of the T_4–T_5 differences being above or below 0.7 K, by comparison with measurements from buoys.

The atmospheric correction algorithms work effectively only in the clear atmosphere. The presence of clouds in the field of view of the infrared radiometer contaminates the measurement so that such pixels must be identified and removed from the SST retrieval process. It is not necessary for the entire pixel to be obscured, even a portion as small as 3–5%, dependent on cloud type and height, can produce unacceptable errors in the SST measurement. Thin, semi-transparent cloud, such as cirrus, can have similar effects to subpixel geometric obscuration by optically thick clouds. Consequently, great attention must be paid in the SST derivation to the identification of measurements contaminated by even a small amount of clouds. This is the principle disadvantage to SST measurement by spaceborne infrared radiometry. Since there are large areas of cloud cover over the open ocean, it may be necessary to composite the cloud-free parts of many images to obtain a complete picture of the SST over an ocean basin.

Similarly, aerosols in the atmosphere can introduce significant errors in SST measurement. Volcanic aerosols injected into the cold stratosphere by violent eruptions produce unmistakable signals that can bias the SST too cold by several degrees. A more insidious problem is caused by less readily identified aerosols at lower, warmer levels of the atmosphere that can introduce systematic errors of a much smaller amplitude.

Microwave Measurements

Microwave radiometers use a similar measurement principle to infrared radiometers, having several spectral channels to provide the information to correct for extraneous effects, and black-body calibration targets to ensure the accuracy of the measurements. The suite of channels is selected to include sensitivity to the parameters interfering with the SST measurements, such as cloud droplets and surface wind speed, which occurs with microwaves at higher frequencies. A simple combination of the brightness temperature, such as eqn [2], can retrieve the SST.

Table 1 Relative merits of infrared and microwave radiometers for sea surface temperature measurement

Infrared	*Microwave*
Good spatial resolution (~ 1 km)	Poor spatial resolution (~ 50 km)
Surface obscured by clouds	Clouds largely transparent, but measurement perturbed by heavy rain
No side-lobe contamination	Side-lobe contamination prevents measurements close to coasts or ice
Aperture is reasonably small; instrument can be compact for spacecraft use	Antenna is large to achieve spatial resolution from polar orbit heights (~800 km above the sea surface)
4 km resolution possible from geosynchronous orbit; can provide rapid sampling data	Distance to geosynchronous orbit too large to permit useful spatial resolution with current antenna sizes

The relative merits of infrared and microwave radiometers for measuring SST are summarized in **Table 1**.

Characteristics of Satellite-derived SST

Because of the very limited penetration depth of infrared and microwave electromagnetic radiation in sea water the temperature measurements are limited to the sea surface. Indeed, the penetration depth is typically less than in the infrared, so that temperature derived from infrared measurements is characteristic of the so-called skin of the ocean. The skin temperature is generally several tenths of a degree cooler than the temperature measured just below, as a result of heat loss from the ocean to atmosphere. On days of high insolation and low wind speed, the absorption of sunlight causes an increase in near surface temperature so that the water just below the skin layer is up to a few degrees warmer than that measured a few meters deeper, beyond the influence of the diurnal heating. For those people interested in a temperature characteristic of a depth of a few meters or more, the decoupling of the skin and deeper, bulk temperatures is perceived as a disadvantage of using satellite SST. However, algorithms generated by comparisons between satellite and *in situ* measurements from buoys include a mean skin effect masquerading as part of the atmospheric effect, and so the application of these results in an estimate of bulk temperatures.

The greatest advantage offered by satellite remote sensing is, of course, coverage. A single, broad-swath,

Table 2 Spectral characteristics of current and planned satellite-borne infrared radiometers

AVHRR		*ATSR*		*MODIS*		*OCTS*		*GLI*	
λ (μm)	*NEΔT (K)*	*λ (μm)*	*NEΔT (K)*	*λ (μm)*	*NEΔT (K)*	*λ (μm)*	*NEΔT (K)*	*λ (μm)*	*NEΔT (K)*
3.75	0.12	3.7	0.019	3.75	0.05	3.7	0.15	3.715	< 0.15
				3.96	0.05				
				4.05	0.05				
				8.55	0.05	8.52	0.15	8.3	< 0.1
10.5	0.12	10.8	0.028	11.03	0.04	10.8	0.15	10.8	< 0.1
11.5	0.12	12.0	0.025	12.02	0.04	11.9	0.15	12	< 0.1

imaging radiometer on a polar-orbiting satellite can provide global coverage twice per day. An imaging radiometer on a geosynchronous satellite can sample much more frequently, once per half-hour for the Earth's disk, or smaller segments every few minutes, but the spatial extent of the data is limited to that part of the globe visible from the satellite.

The satellite measurements of SST are also reasonably accurate. Current estimates for routine measurements show absolute accuracies of ± 0.3 to ± 0.5 K when compared to similar measurements from ships, aircraft, and buoys.

Spacecraft Instruments

All successful instruments have several attributes in common: a mechanism for scanning the Earth's surface to generate imagery, good detectors, and a mechanism for real-time, in-flight calibration. Calibration involves the use of one or more black-body calibration targets, the temperatures of which are accurately measured and telemetered along with the imagery. If only one black-body is available a measurement of cold dark space provides the equivalent of a very cold calibration target. Two calibration points are needed to provide in-flight calibration; nonlinear behavior of the detectors is accounted for by means of pre-launch instrument characterization measurements.

The detectors themselves inject noise into the data stream, at a level that is strongly dependent on their temperature. Therefore, infrared radiometers require cooled detectors, typically operating from 78 K (-195°C) to 105 K (-168°C) to reduce the noise equivalent temperature difference (NEΔT) to the levels shown in **Table 2**.

The Advanced Very High Resolution Radiometer (AVHRR)

The satellite instrument that has contributed the most to the study of the temperature of the ocean surface is the AVHRR that first flew on TIROS-N launched in late 1978. AVHRRs have flown on successive satellites of the NOAA series from NOAA-6 to NOAA-14, with generally two operational at any given time. The NOAA satellites are in a near-polar, sun-synchronous orbit at a height of about 780 km above the Earth's surface and with an orbital period of about 100 min. The overpass times of the two NOAA satellites are about 2.30 a.m. and p.m. and about 7.30 a.m. and p.m. local time. The AVHRR has five channels: 1 and 2 at ~ 0.65 and ~ 0.85 μm are responsive to reflected sunlight and are used to detect clouds and identify coastlines in the images from the daytime part of each orbit. Channels 4 and 5 (**Table 2** and **Figure 1**) are in the atmospheric window close to the peak of the thermal emission from the sea surface and are used primarily for the measurement of sea surface temperature. Channel 3, positioned at the shorter wavelength atmospheric window, is responsive to both surface emission and reflected sunlight. During the nighttime part of each orbit, measurements of channel 3 brightness temperatures can be used with those from channels 4 and 5 in variants of the atmospheric correction algorithm to determine SST. The presence of reflected sunlight during the daytime part of the orbit prevents much of these data from being used for SST measurement. Because of the tilting of the sea surface by waves, the area contaminated by reflected sunlight (sun glitter) can be quite extensive, and is dependent on the local surface wind speed. It is limited to the point of specular reflection only in very calm seas.

The images in each channel are constructed by scanning the field of view of the AVHRR across the Earth's surface by a mirror inclined at 45° to the direction of flight (**Figure 2A**). The rate of rotation, 6.67 Hz, is such that successive scan lines are contiguous at the surface directly below the satellite. The width of the swath (~ 2700 km) means that the swaths from successive orbits overlap so that the whole Earth's surface is covered without gaps each day.

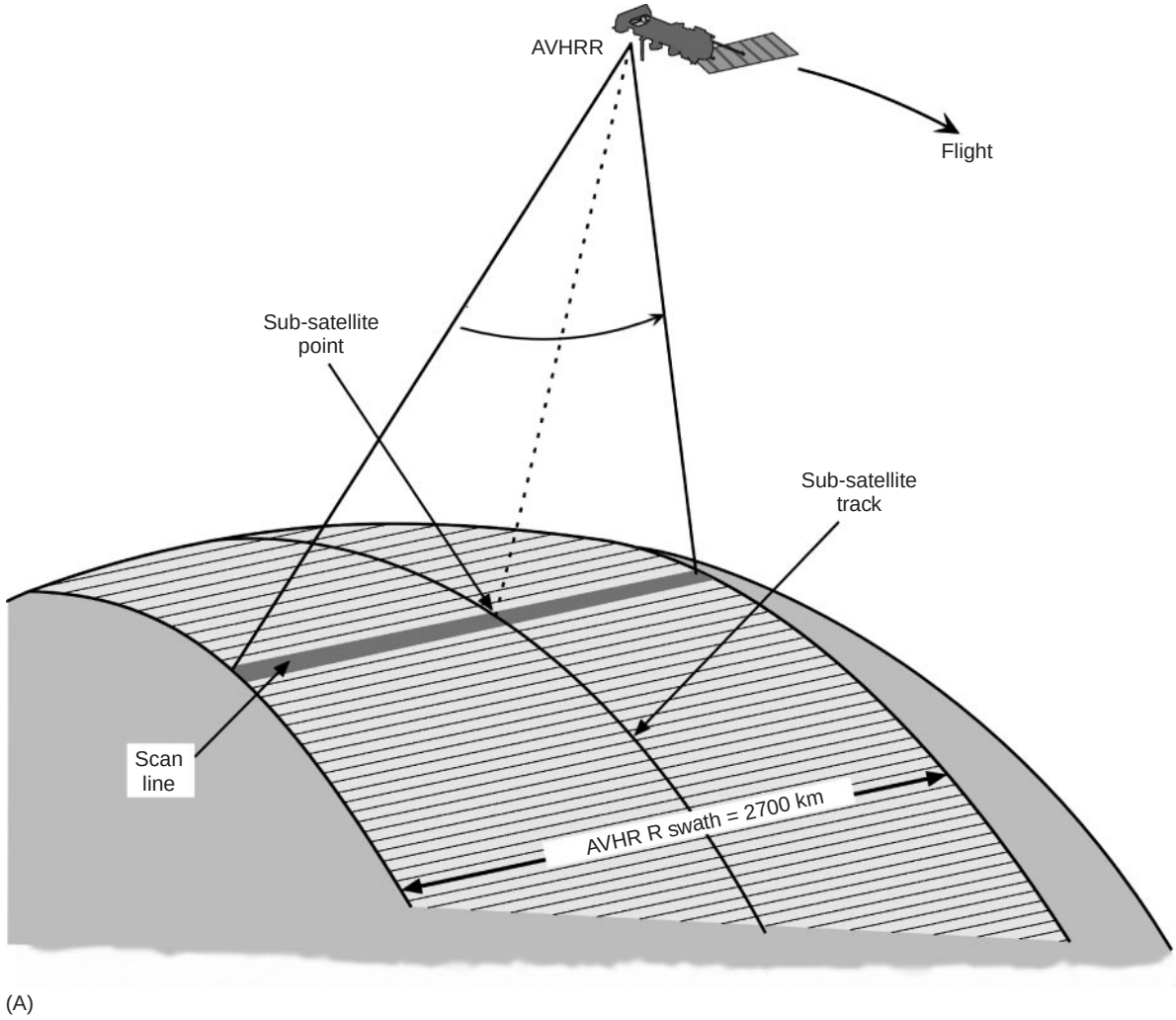

Figure 2 Scan geometries of AVHRR (A) and ATSR (B). The continuous wide swath of the AVHRR is constructed by linear scan lines aligned across the direction of motion of the subsatellite point. The swaths of the ATSR are generated by an inclined conical scan, which covers the same swath through two different atmospheric path lengths. The swath is limited to 512 km by geometrical constraints. Both radiometers are on sun-synchronous, polar-orbiting satellites.

The Along-Track Scanning Radiometer (ATSR)

An alternative approach to correcting the effects of the intervening atmosphere is to make a brightness temperature measurement of the same area of sea surface through two different atmospheric path lengths. The pairs of such measurements must be made in quick succession, so that the SST and atmospheric conditions do not change in the time interval. This approach is that used by the ATSR, two of which have flown on the European satellites ERS-1 and ERS-2.

The ATSR has infrared channels in the atmospheric windows comparable to those of AVHRR, but the rotating scan mirror sweeps out a cone inclined from the vertical by its half-angle (**Figure 2B**). The field of view of the ATSR sweeps out a curved path on the sea surface, beginning at the point directly below the satellite, moving out sideways and forwards. Half a mirror revolution later, the field of view is about 900 km ahead of the subsatellite track in the center of the 'forward view'. The path of the field of view returns to the subsatellite point, which, during the period of the mirror rotation, has moved 1 km ahead of the starting point. Thus the pixels forming the successive swaths through the nadir point are contiguous. The orbital motion of the satellite means that the nadir point overlays the center of the forward view after about 2 min. The atmospheric path length of the measurement at nadir is simply the thickness of the atmosphere, whereas the slant path to the center of the

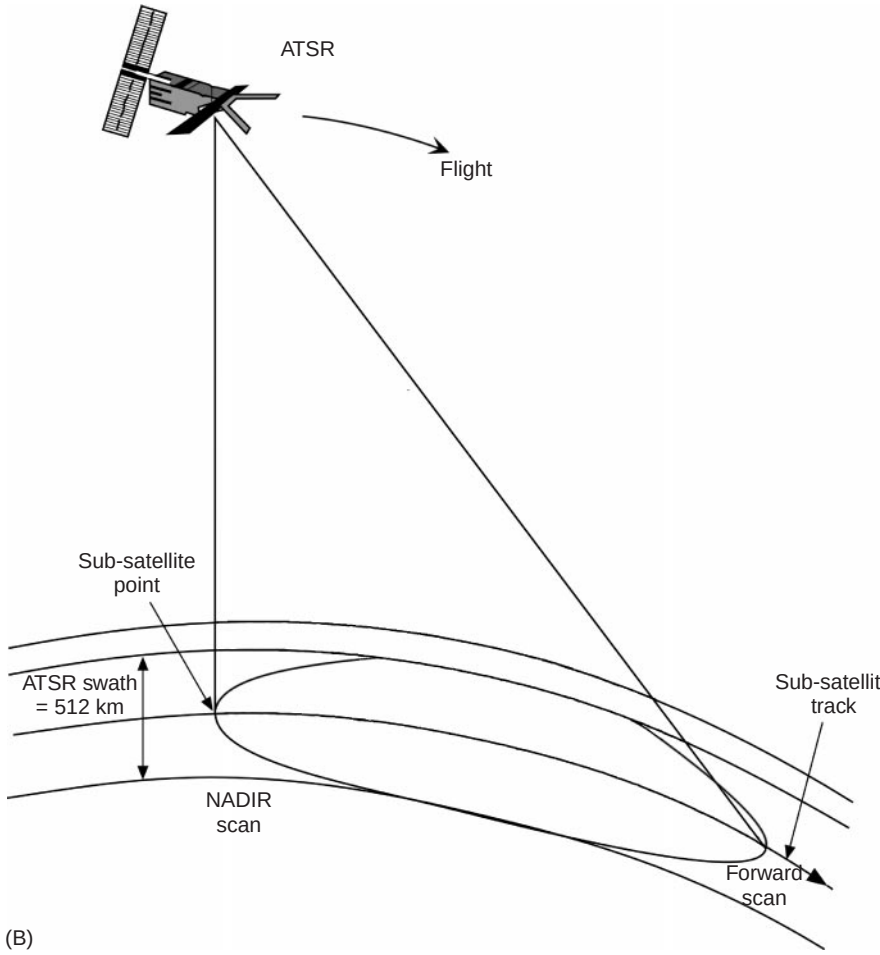

Figure 2 *Continued*

forward view is almost double that, resulting in colder brightness temperatures. The differences in the brightness temperatures between the forward and nadir swaths are a direct measurement of the effect of the atmosphere and permit a more accurate determination of the sea surface temperature. The atmospheric correction algorithm takes the form:

$$SST = c_o + \sum_i c_{n,i} T_{n,i} + \sum_i c_{f,i} T_{f,i} \qquad [5]$$

where the subscripts n and f refer to measurements from the nadir and forward views, i indicates two or three atmospheric window channels and the set of c are coefficients. The coefficients, derived by radiative transfer simulations, have an explicit latitudinal dependence.

Accurate calibration of the brightness temperatures is achieved by using two onboard black-body cavities, situated between the apertures for the nadir and forward views such that they are scanned each rotation of the mirror. One calibration target is at the spacecraft ambient temperature while the other is heated, so that the measured brightness temperatures of the sea surface are straddled by the calibration temperatures.

The limitation of the simple scanning geometry of the ATSR is a relatively narrow swath width of 512 km. The ERS satellites have at various times in their missions been placed in orbits with repeat patterns of 3, 35, and 168 days, and given the narrow ATSR swath, complete coverage of the globe has been possible only for the 35 and 186 day cycles. This disadvantage is offset by the intended improvement in absolute accuracy of the atmospheric correction, and of its better insensitivity to aerosol effects.

The Moderate Resolution Imaging Spectroradiometer (MODIS)

The MODIS is a 36-band imaging radiometer on the NASA Earth Observing System (EOS) satellites *Terra*, launched in December 1999, and *Aqua*, planned for launch by late 2001. MODIS is much more

complex than other radiometers used for SST measurement, but uses the same atmospheric windows. In addition to the usual two bands in the 10–12 μm interval, MODIS has three narrow bands in the 3.7–4.1 μm windows, which, although limited by sun-glitter effects during the day, hold the potential for much more accurate measurement of SST during the night. Several of the other 31 bands of MODIS contribute to the SST measurement by better identification of residual cloud and aerosol contamination.

The swath width of MODIS, at 2330 km, is somewhat narrower than that of AVHRR, with the result that a single day's coverage is not entire, but the gaps from one day are filled in on the next. The spatial resolution of the infrared window bands is 1 km at nadir.

The GOES Imager

SST measurements from geosynchronous orbit are made using the infrared window channels of the GOES Imager. This is a five-channel instrument that remains above a given point on the Equator. The image of the Earth's disk is constructed by scanning the field of view along horizontal lines by an oscillating mirror. The latitudinal increments of the scan line are done by tilting the axis of the scan mirror. The spatial resolution of the infrared channels is 2.3 km (east–west) by 4 km (north–south) at the subsatellite point. There are two imagers in orbit at the same time on the two GOES satellites, covering the western Atlantic Ocean (GOES-East) and the eastern Pacific Ocean (GOES-West). The other parts of the global oceans visible from geosynchronous orbit are covered by three other satellites operated by Japan, India, and the European Meteorological Satellite organization (Eumetsat). Each carries an infrared imager, but with lesser capabilities than the GOES Imager.

TRMM Microwave Imager (TMI)

The TMI is a nine-channel microwave radiometer on the Tropical Rainfall Measuring Mission satellite, launched in 1997. The nine channels are centered at five frequencies: 10.65, 19.35, 21.3, 37.0, and 85.5 GHz, with four of them being measured at two polarizations. The 10.65 GHz channels confer a sensitivity to SST, at least in the higher SST range found in the tropics, that has been absent in microwave radiometers since the SMMR (Scanning Multifrequency Microwave Radiometer) that flew on the short-lived Seasat in 1978 and on Nimbus-7 from 1978 to 1987. Although SSTs were derived from SMMR measurements, these lacked the spatial resolution and absolute accuracy to compete with those of the AVHHR. The TMI complements AVHRR data by providing SSTs in the tropics where persistent clouds can be a problem for infrared retrievals. Instead of a rotating mirror, TMI, like other microwave imagers, uses an oscillating parabolic antenna to direct the radiation through a feed-horn into the radiometer.

The swath width of TMI is 759 km and the orbit of TRMM restricts SST measurements to within 38.5° of the equator. The beam width of the 10.65 GHz channels produces a footprint of 37×63 km, but the data are over-sampled to produce 104 pixels across the swath.

Applications

With absolute accuracies of satellite-derived SST fields of ~ 0.5 K or better, and even smaller relative uncertainties, many oceanographic features are resolved. These can be studied in a way that was hitherto impossible. They range from basin-scale perturbations to frontal instabilities on the scales of tens of kilometers. SST images have revealed the great complexity of ocean surface currents; this complexity was suspected from shipboard and aircraft measurements, and by acoustically tacking neutrally buoyant floats. However, before the advent of infrared imagery the synoptic view of oceanic variability was elusive, if not impossible.

El Niño

The El Niño Southern Oscillation (ENSO) phenomenon has become a well-known feature of the coupled ocean–atmosphere system in terms of perturbations that have a direct influence on people's lives, mainly by altering the normal rainfall patterns causing draughts or deluges – both of which imperil lives, livestock, and property.

The normal SST distribution in the topical Pacific Ocean is a region of very warm surface waters in the west, with a zonal gradient to cooler water in the east; superimposed on this is a tongue of cool surface water extending westward along the Equator. This situation is associated with heavy rainfall over the western tropical Pacific, which is in turn associated with lower level atmospheric convergence and deep atmospheric convection. The atmospheric convergence and convection are part of the large-scale global circulation. The warm area of surface water, enclosed by the 28°C isotherm, is commonly referred to as the 'Warm Pool' and in the normal situation is confined to the western part of the tropical Pacific. During an El Niño event the warm

surface water, and associated convection and rainfall, migrate eastward perturbing the global atmospheric circulation. El Niño events occur up to a few times per decade and are of very variable intensity. Detailed knowledge of the shape, area, position, and movement of the Warm Pool can be provided from satellite-derived SST to help study the phenomenon and forecast its consequences.

Figure 3 shows part of the global SST fields derived from the Pathfinder SST algorithm applied to AVHRR measurements. The tropical Pacific SST field in the normal situation (December 1993) is shown in the upper panel, while the lower panel shows the anomalous field during the El Niño event of 1997–98. This was one of the strongest El Niños on record, but also the best documented and forecast. Seasonal predictions of disturbed patterns of winds and rainfall had an unprecedented level of accuracy and provided improved useful forecasts for agriculture in many affected areas. Milder than usual hurricane and tropical cyclone seasons were successfully forecast, as were much wetter winters and severe coastal erosion on the Pacific coasts of the Americas.

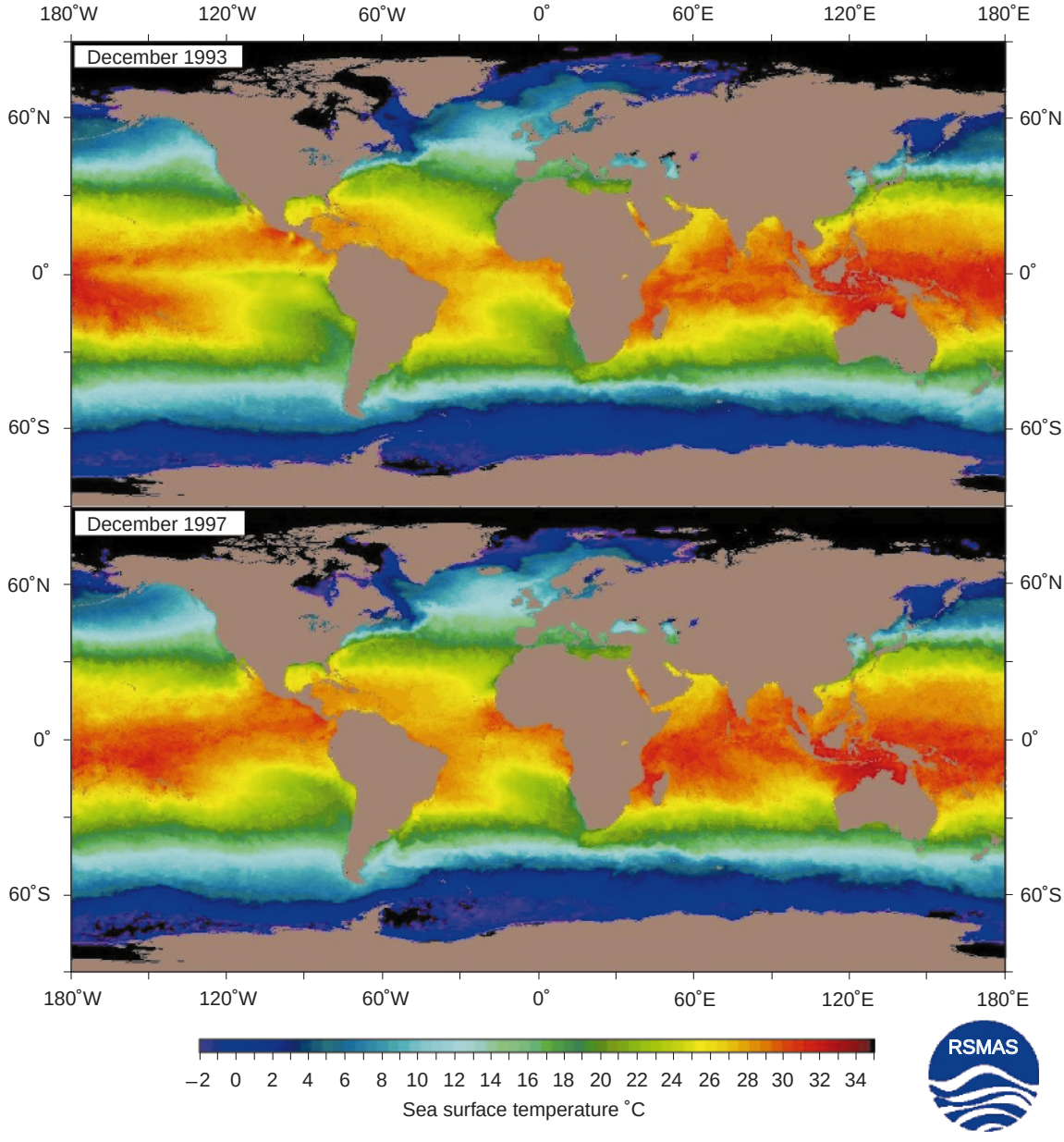

Figure 3 Global maps of SST derived from the AVHRR Pathfinder data sets. These are monthly composites of cloud-free pixels and show the normal situation in the tropical Pacific Ocean (above) and the perturbed state during an El Niño event (below).

Hurricane Intensification

The Atlantic hurricane season in 1999 was one of the most damaging on record in terms of land-falling storms in the eastern USA, Caribbean, and Central America. Much of the damage was not a result of high winds, but of torrential rainfall. Accurate forecasting of the path and intensity of these land-falling storms is very important, and a vital component of this forecasting is detailed knowledge of SST patterns in the path of the hurricanes. The SST is indicative of the heat stored in the upper ocean that is available to intensify the storms, and SSTs of $> 26^{\circ}C$ appear to be necessary to trigger the intensification of the hurricanes. Satellite-derived SST maps are used in the prediction of the development of storm propagation across the Atlantic Ocean from the area off Cape Verde where atmospheric disturbances spawn the nascent storms. Closer to the USA and Caribbean, the SST field is important in determining the sudden intensification that can occur just before landfall. After the hurricane has passed, they sometimes leave a wake of cooler water in the surface that is readily identifiable in the satellite-derived SST fields.

Frontal Positions

One of the earliest features identified in infrared images of SST were the positions of ocean fronts, which delineate the boundaries between dissimilar surface water masses. Obvious examples are western boundary currents, such as the Gulf Stream in the Atlantic Ocean (**Figure 4**) and the Kuroshio in the Pacific Ocean, both of which transport warm surface water poleward and away from the western coastlines. In the Atlantic, the path of the warm surface water of the Gulf Stream can be followed in SST images across the ocean, into the Norwegian Sea, and into the Arctic Ocean. The surface water loses heat to the atmosphere, and to adjacent cooler waters on this path from the Gulf of Mexico to the Arctic, producing a marked zonal difference in the climates of the opposite coasts of the Atlantic and Greenland-Norwegian Seas. Instabilities in the fronts at the sides of the currents have been revealed in great detail in the SST images. Some of the large-scale instabilities can lead to loops on scales of a few tens to hundreds of kilometers that can become 'pinched off' from the flow and evolve as independent features, migrating away from the currents. When these occur on the equator side of the current these are called 'Warm Core Rings' and can exist for many months; in the case of the Gulf Stream these can propagate into the Sargasso Sea.

Figure 5 shows a series of instabilities along the boundaries of the Equatorial current system in the Pacific Ocean. The extent and structure of these features were first described by analysis of satellite SST images.

Coral Bleaching

Elevated SSTs in the tropics have adverse influences on living coral reefs. When the temperatures exceed the local average summertime maximum for several days, the symbiotic relationship between the coral polyps and their algae breaks down and the reef-building animals die. The result is extensive areas where the coral reef is reduced to the skeletal structure without the living and growing tissue, giving the reef a white appearance. Time-series of AVHRR-derived SST have been shown to be valuable predictors of reef areas around the globe that are threatened by warmer than usual water temperatures. Although it is not possible to alter the outcome, SST maps have been useful in determining the scale of the problem and identifying threatened, or vulnerable reefs.

The 'Global Thermometer'

Some of the most pressing problems facing environmental scientists are associated with the issue of global climate change: whether such changes are natural or anthropogenic, whether they can be forecast accurately on regional scales over decades, and whether undesirable consequences can be avoided. The past decade has seen many air temperature records being surpassed and indeed the planet appears to be warming on a global scale. However, the air temperature record is rather patchy in its distribution, with most weather stations clustered on Northern Hemisphere continents.

Global SST maps derived from satellites provide an alternative approach to measuring the Earth's temperature in a more consistent fashion. However, because of the very large thermal inertia of the ocean (it takes as much heat to raise the temperature of only the top meter of the ocean through one degree as it does for the whole atmosphere), the SST changes indicative of global warming are small. Climate change forecast models indicate a rate of temperature increase of only a few tenths of a degree per decade, and this is far from certain because of our incomplete understanding of how the climate system functions, especially in terms of various feedback factors such as those involving changes in cloud and aerosol properties. Such a rate of temperature increase will require SST records of several decades length before the signal, if present, can be unequivocally identified above the

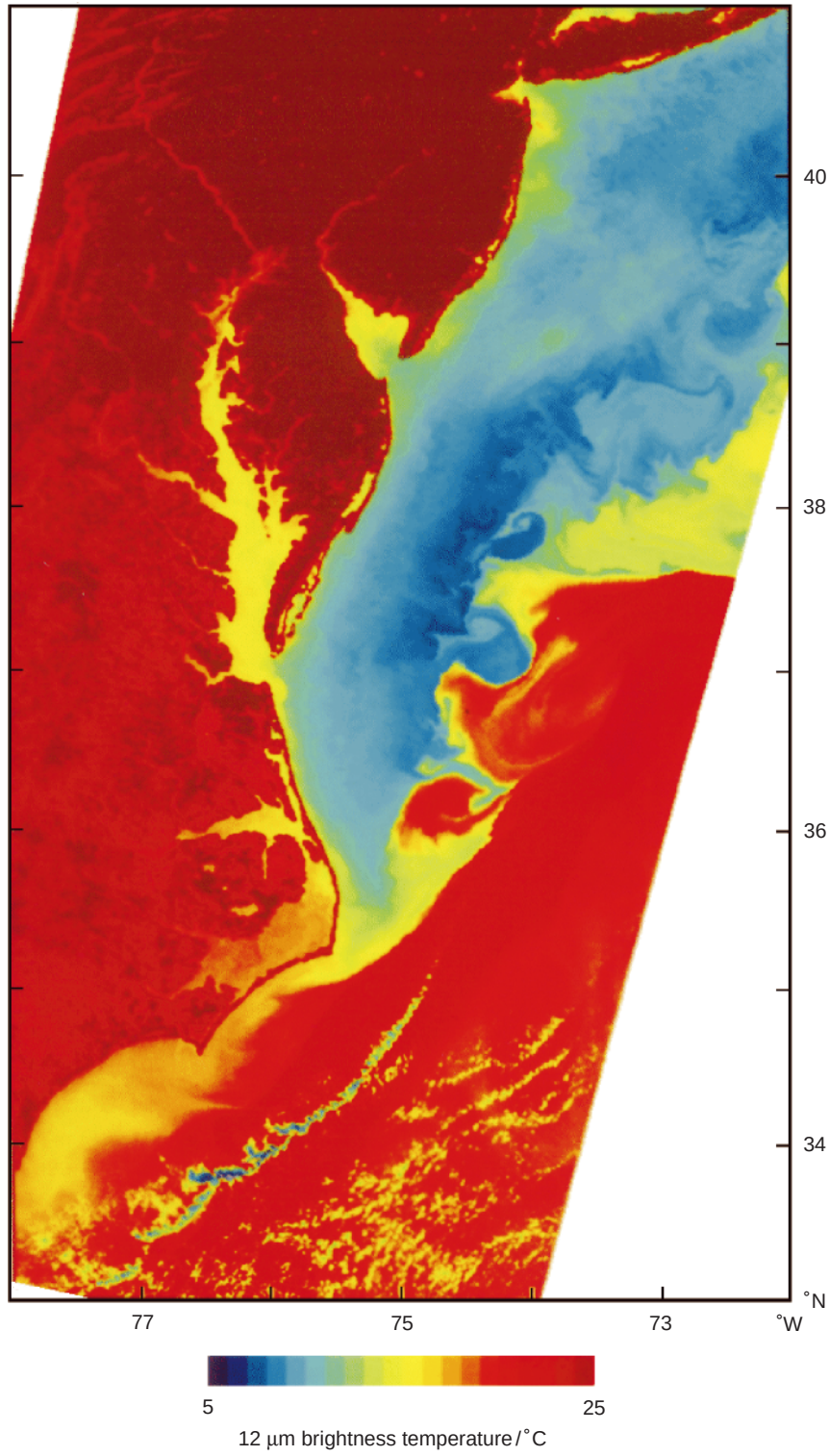

Figure 4 Brightness temperature image derived from the measurements of the ATSR on a nearly cloud-free day over the eastern coast of the USA. The warm core of the Gulf Stream is very apparent; it departs from the coast at Cape Hatteras. The cool, shelf water from the north entrains the warmer outflows from the Chesapeake and Delaware Bays. The north wall of the Gulf Stream reveals very complex structure associated with frontal instabilities that lead to exchanges between the Gulf Stream and inshore waters. The small-scale multicolored patterns over the warm Gulf Stream waters to the south indicate the presence of cloud. This image was taken at 15.18 UTC on 21 May 1992, and is derived from nadir view data from the 12 μm channel. (Generated from data © NERC/ESA/RAL/BNSC, 1992.)

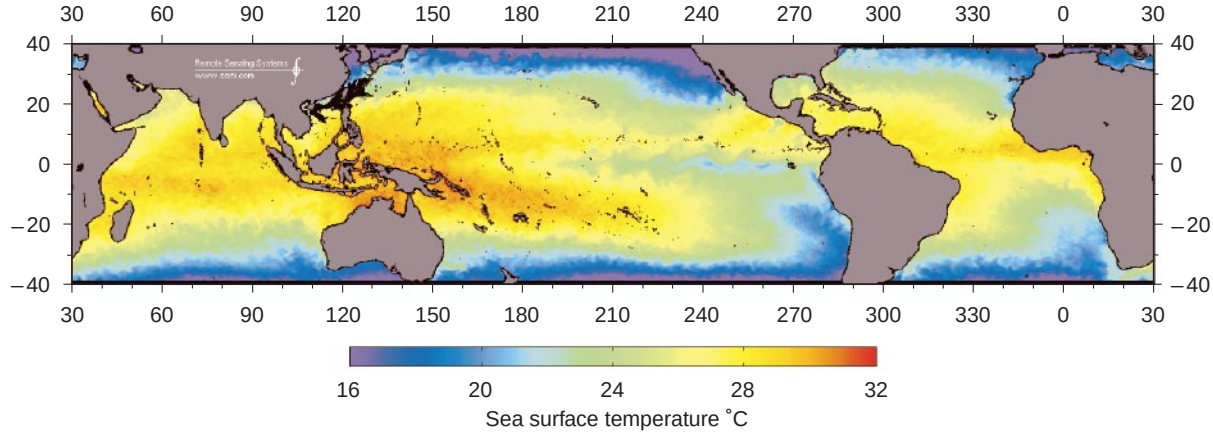

Figure 5 Tropical SSTs produced by microwave radiometer measurements from the TRMM (Tropical Rainfall Measuring Mission) Microwave Imager (TMI). This is a composite generated from data taken during the week ending December 22, 1999. The latitudinal extent of the data is limited by the orbital geometry of the TRMM satellite. The measurement is much less influenced by clouds than those in the infrared, but the black pixels in parts of the oceans where there are no islands indicate areas of heavy rainfall. The image reveals the cold tongue of surface water along the Equator in the Pacific Ocean and cold water off the Pacific coast of South America, indicating a non-El Niño situation. Note that the color scale is different from that used in **Figure 3**. The image was produced by Remote Sensing Systems, sponsored in part by NASA'S Earth Science Information Partnerships (ESIP) (a federation of information sites for Earth science); and by the NOAA/NASA Pathfinder Program for early EOS products; principal investigator: Frank Wentz.

uncertainties in the accuracy of the satellite-derived SSTs. Furthermore, the inherent natural variability of the global SST fields tends to mask any small, slow changes. Difficult though this task may be, global satellite-derived SSTs are an important component in climate change research.

Air-sea Exchanges

The SST fields play further indirect roles in the climate system in terms of modulating the exchanges of heat and greenhouse gases between the ocean and atmosphere. Although SST is only one of several variables that control these exchanges, the SST distributions, and their evolution on seasonal timescales can help provide insight into the global patterns of the air–sea exchanges. An example of this is the study of tropical cloud formation over the ocean, a consequence of air–sea heat and moisture exchange, in terms of SST distributions.

Future Developments

Over the next several years continuing improvement of the atmospheric correction algorithms can be anticipated to achieve better accuracies in the derived SST fields, particularly in the presence of atmospheric aerosols. This will involve the incorporation of information from additional spectral channels, such as those on MODIS or other EOS era satellite instruments. Improvements in SST coverage, at least in the tropics, can be expected in areas of heavy, persistent cloud cover by melding SST retrievals from high-resolution infrared sensors with those from microwave radiometers, such as the TMI.

Continuing improvements in methods of validating the SST retrieval algorithms will improve our understanding of the error characteristics of the SST fields, guiding both the appropriate applications of the data and also improvements to the algorithms.

On the hardware front, a new generation of infrared radiometers designed for SST measurements will be introduced on the new operational satellite series, the National Polar-Orbiting Environmental Satellite Environments System (NPOESS) that will replace both the civilian (NOAA-n) and military (DMSP, Defense Meteorological Satellite Program) meteorological satellites. The new radiometer, called VIIRS (the Visible and Infrared Imaging Radiometer Suite), will replace the AVHRR and MODIS. The prototype VIIRS will fly on the NPP (NPOESS Preparatory Program) satellite scheduled for launch in late 2005. At present, the design details of the VIIRS are not finalized, but the physics of the measurement constrains the instrument to use the same atmospheric window channels as previous and current instruments, and have comparable, or better, measurement accuracies.

The ATSR series will continue with at least one more model, called the Advanced ATSR (AATSR) to fly on Envisat to be launched in 2001. The SST capability of this will be comparable to that of its predecessors.

Thus, the time-series of global SSTs that now extends for two decades will continue into the

future to provide invaluable information for climate and oceanographic research.

See also

Air–Sea Gas Exchange. Carbon Dioxide (CO_2) Cycle. Coral Reef and other Tropical Fisheries. Current Systems in the Indian Ocean. Current Systems in the Southern Ocean. Dispersion in Shallow Seas. Electrical Properties of Sea Water. El Niño Southern Oscillation (ENSO). Evaporation and Humidity. Heat and Momentum Fluxes at the Sea Surface. IR Radiometers. Ocean Circulation. Ocean Color from Satellites. Penetrating Shortwave Radiation. Radiative Transfer in the Ocean. Satellite Altimetry. Satellite Measurements of Salinity. Satellite Oceanography, History and Introductory Concepts. Satellite Remote Sensing SAR. Shelf-sea and Slope Fronts. Thermohaline Circulation. Upper Ocean Time and Space Variability.

Further Reading

Barton IJ (1995) Satellite-derived sea surface temperatures: Current status. *Journal of Geophysical Research* 100: 8777–8790.

Gurney RJ, Foster JL and Parkinson CL (eds) (1993) *Atlas of Satellite Observations Related to Global Change*. Cambridge: Cambridge University Press.

Ikeda M and Dobson FW (1995) *Oceanographic Applications of Remote Sensing*. London: CRC Press.

Kearns EJ, Hanafin JA, Evans RH, Minnett PJ and Brown OB (2000) An independent assessment of Pathfinder AVHRR sea surface temperature accuracy using the Marine-Atmosphere Emitted Radiance Interferometer (M-AERI). Bulletin of the American Meteorological Society. 81: 1525–1536.

Kidder SQ and Vonder Haar TH (1995) *Satellite Meteorology: An Introduction*. London: Academic Press.

Legeckis R and Zhu T (1997) Sea surface temperature from the GEOS-8 geostationary satellite. *Bulletin of the American Meteorological Society* 78: 1971–1983.

May DA, Parmeter MM, Olszewski DS and Mckenzie BD (1998) Operational processing of satellite sea surface temperature retrievals at the Naval Oceanographic Office. *Bulletin of the American Meteorological Society*, 79: 397–407.

Robinson IS (1985) *Satellite Oceanography: An Introduction for Oceanographers and Remote-sensing Scientists*. Chichester: Ellis Horwood.

Stewart RH (1985) *Methods of Satellite Oceanography*. Berkeley, CA: University of California Press.

Victorov S (1996) *Regional Satellite Oceanography*. London: Taylor and Francis.

SATELLITE REMOTE SENSING SAR

A. K. Liu and S. Y. Wu, NASA Goddard Space Flight Center, Greenbelt, MD, USA

doi:10.1006/rwos.2001.0339

Introduction

Synthetic aperture radar (SAR) is a side-looking imaging radar usually operating on either an aircraft or a spacecraft. The radar transmits a series of short, coherent pulses to the ground producing a footprint whose size is inversely proportional to the antenna size, its aperture. Because the antenna size is generally small, the footprint is large and any particular target is illuminated by several hundred radar pulses. Intensive signal processing involving the detection of small Doppler shifts in the reflected signals from targets to the moving radar produces a high resolution image that is equivalent to one that would have been collected by a radar with a much larger aperture. The resulting larger aperture is the 'synthetic aperture' and is equal to the distance traveled by the spacecraft while the radar antenna is collecting information about the target. SAR techniques depend on precise determination of the relative position and velocity of the radar with respect to the target, and on how well the return signal is processed.

SAR instruments transmit radar signals, thus providing their own illumination, and then measure the strength and phase of the signals scattered back to the instrument. Radar waves have much longer wavelengths compared with light, allowing them to penetrate clouds with little distortion. In effect, radar's longer wavelengths average the properties of air with the properties and shapes of many individual water droplets, and are only affected while entering and exiting the cloud. Therefore, microwave radar can 'see' through clouds.

SAR images of the ocean surface are used to detect a variety of ocean features, such as refracting surface gravity waves, oceanic internal waves, wind fields, oceanic fronts, coastal eddies, and intense low pressure systems (i.e. hurricanes and polar lows), since they all influence the short wind waves responsible for radar backscatter. In addition, SAR is the only sensor that provides measurements of the